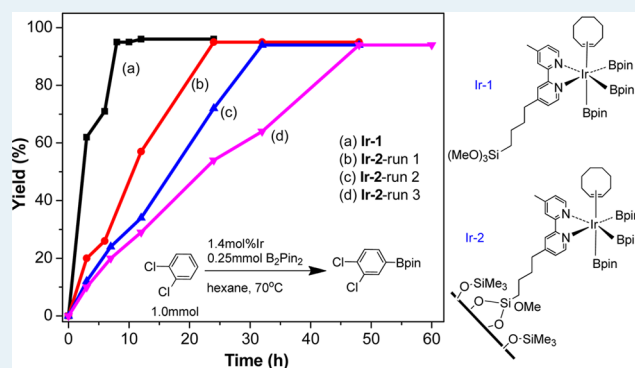


Recyclable Silica-Supported Iridium Bipyridine Catalyst for Aromatic C–H Borylation

Fengshou Wu,^{†,‡,§} Yan Feng,^{†,§} and Christopher W. Jones^{*,†}[†]School of Chemical & Biomolecular Engineering, Georgia Institute of Technology, 311 Ferst Drive NW, Atlanta, Georgia 30332, United States[‡]College of Chemistry and Molecular Sciences, Wuhan University, Wuhan, Hubei, 430072, P. R. China**S** Supporting Information

ABSTRACT: A mesoporous silica (SBA-15)-supported bipyridine iridium complex is prepared by grafting of bipyridine onto the silica support, followed by complexation of an iridium(I) precursor in the presence of HBpin and cyclooctene. Structural analyses by X-ray powder diffraction, nitrogen physisorption, FT-IR, and solid-state NMR spectroscopy demonstrate that the 3-dimensional, hexagonal pore structure of SBA-15 is maintained after the immobilization. In particular, as a heterogeneous catalyst, this silica-supported iridium complex shows moderate to good catalytic activity in the aromatic C–H borylation of a variety of substrates. More importantly, the heterogeneous catalyst is recovered easily and reused repeatedly by simple washing without chemical treatment and exhibits good recycling performance with a modest decrease in the catalytic rate, showing good potential for increasing the overall turnover number of this synthetically useful catalyst.

KEYWORDS: iridium, heterogeneous catalysis, recyclable, immobilization, mesoporous materials, arenes, C–H borylation



1. INTRODUCTION

Arylboronic acids and their derivatives are very important intermediates in organic synthesis.¹ Among the routes to arylboronic acid derivatives, direct C–H borylation of arenes is the most attractive.² Since the first catalysts for the direct borylation of arenes based on Cp*Ir complexes were reported by Smith and co-workers,³ various iridium systems containing phosphine- and nitrogen-based ligands have been studied.⁴ In 2002, Ishiyama, Hartwig, and co-workers reported the borylation of arenes catalyzed by bipyridine iridium complexes.⁵ Concurrently, catalysts based on iridium phosphine complexes were reported by Smith, Maleczka, and co-workers.² Generally, catalysts containing bipyridine derivatives are more reactive for most borylations of arenes compared with those containing phosphine ligands.⁶ Studies of the precatalysts such as (η^6 -mesitylene)Ir(Bpin)₃ and (dtbpy)Ir(Bpin)₃(coe) (dtbpy = 4,4'-di-*tert*-butyl-2,2'-bipyridine, coe = cyclooctene) support a mechanism in which species of the formula L₂Ir^{III}Bpin₃ are the intermediates that mediate C–H cleavage.^{5,7} A valence cycle between Ir^{III} and Ir^V was involved during the process of the aryl borylation (Scheme 1).^{7d} After much experimentation by Hartwig and co-workers, (dtbpy)Ir(Bpin)₃(coe) was isolated in 80–95% yield.^{7c}

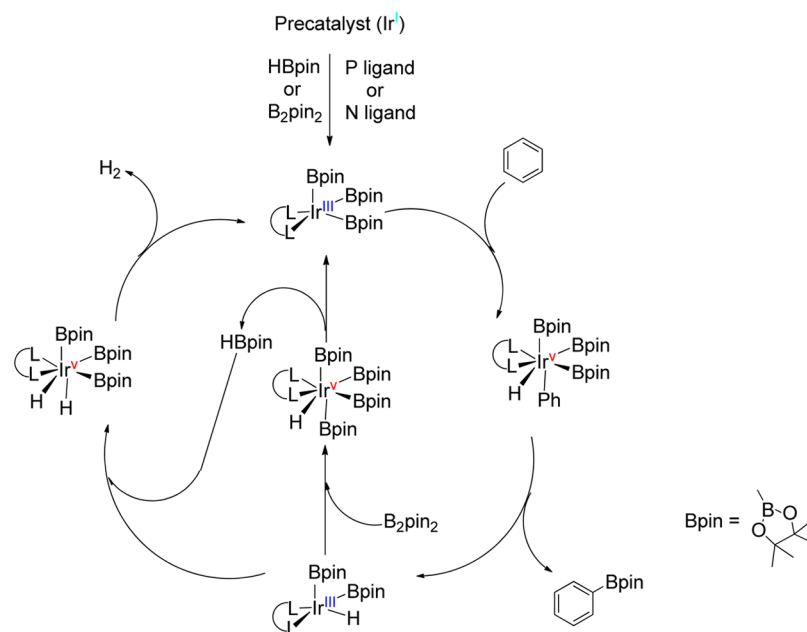
However, direct C–H borylation is usually catalyzed by iridium complexes in a homogeneous mode of operation, which shares common drawbacks, that is, catalyst recovery and recycling is difficult. To this end, in cases that stable catalysts

can be prepared, heterogeneous catalytic systems are attractive. In 2007, Zhu et al. synthesized ionic liquid-stabilized iridium(0) nanoparticles that could be used as catalysts for the C–H borylation of arenes by pinacolborane (HBpin).⁸ These catalytic systems were reused six times; however, the catalyst was difficult to recover because the products first had to be separated from the reaction mixture by distillation. In 2009, Nishida and co-workers obtained an insoluble iridium complex by filtration from the reaction mixtures of 2,2'-bipyridine-4,4'-dicarboxylic acid, [IrCl(cod)]₂ and bis(pinacolato)diboron. The iridium catalyst could be reused 10 times over 1 week in aromatic C–H borylation reactions. However, the structure of this iridium complex was unconfirmed because of its instability under air and its insolubility in organic media.⁹ In the same year, Sawamura and co-workers reported a supported catalyst for aryl borylation.¹⁰ Their studies showed that reaction of B₂pin₂ with methylbenzoates catalyzed by the combination of [Ir(cod)(OMe)]₂ and a silica-supported phosphine ligand resulted in ortho-directed aromatic borylation in excellent yields. Subsequently, similar reactions were studied with HBpin as the boron reagent using the same catalyst.¹¹ However, the supported Ir^I complex purported to form during the reaction

Received: October 21, 2013

Revised: March 25, 2014

Published: March 25, 2014

Scheme 1. Proposed Mechanisms for Ir-Catalyzed Aromatic C–H Borylation^{6,7d}

was not actually isolated because it is not air stable, especially under moist conditions.^{7d}

In parallel, they also reported a similar supported phosphine-Rh system based on [Rh(OH)(cod)]₂. This Rh catalysis was effective for arenes with oxygen-based directing groups, complementing the Ir-catalyzed orthoborylation.¹² Like the supported phosphine-iridium systems, recycling tests were not studied for this rhodium catalyst. In related work, Westcott et al. also reported a supported phosphine-Rh system for olefin hydroboration in which reactions with simple vinyl arenes (ArCH=CH₂) and catecholborane (HBcat) catalyzed by Rh(acac)(coe)₂ (acac = acetylacetonato)/silica-diphenylphosphine could give selective formation of the corresponding branched isomers [ArCH(Bcat)Me].¹³ The immobilized rhodium complex recovered by filtration from the reaction mixtures could be reused, although little is known about the structure of this supported catalyst. Thus, a more convenient catalyst for borylation reactions that is air-stable and easier to recover and reuse would be a useful advance.

In this context, here, we describe a new silica-supported iridium complex for C–H borylation catalysis. Specifically, we have developed an immobilized bipyridine-iridium system prepared from a silica-supported bipyridine ligand and an Ir(I) precursor [Ir(cod)(OMe)]₂. Mesoporous silica SBA-15 was chosen as a support for the iridium complex because of its advantageous properties, such as excellent chemical and thermal stability, high porosity, large surface area, and high surface concentration of silanols, that are useful for silane grafting. The synthesized silica-supported iridium complex was characterized in detail to elucidate its structure using a combination of methods, such as NMR spectroscopy, IR spectroscopy, nitrogen physisorption, XRD, elemental analysis, and TGA. In parallel, an analogous unsupported iridium complex was also prepared for comparison using a similar method. The catalytic results showed that both the unsupported catalyst (Ir-1) and supported catalyst (Ir-2) exhibit moderate to good activity for the borylation of various arenes containing different kinds of functional groups. Furthermore, recycling studies revealed that the heterogeneous

catalyst is highly stable in air and can be reused several times without significantly affecting the structure or the texture of the catalyst.

2. MATERIALS AND METHODS

2.1. General. Solution ¹H and ¹³C NMR spectra were recorded on a Mercury VX 400 MHz instrument. Solid-state ¹³C and ²⁹Si cross-polarization magic angle spinning (CP-MAS) NMR spectra and ¹¹B MAS NMR (B₀ = 9.40 T, ν_L(¹¹B) = 128.38 MHz) spectra were collected on Bruker DSX 300 or 400 MHz instruments. Mass spectra were recorded with a VG 7070 EQ-HF hybrid tandem mass spectrometer or an Applied Biosystems 4700 spectrometer. Iridium and silicon elemental analyses were performed by Columbia Analytical Services (Tucson, AZ, USA), using ICP-AES. Carbon, hydrogen, and nitrogen contents were determined via CHN analysis, also by Columbia Analytical Services. Thermogravimetric analysis (TGA) was performed on a Netzsch STA409, and the ligand loading was calculated from relative weight loss in the range 150–400 °C. X-ray powder diffraction was performed on a PAnalytical X'Pert Pro diffractometer with a Cu Kα source. The nitrogen (N₂) adsorption–desorption isotherms were measured on a Micromeritics Tristar 2030 at 77 K. The samples were outgassed at 110 °C overnight before the measurements. The surface areas were determined on the basis of the Brunauer–Emmett–Teller (BET) method, and the total pore volumes and pore sizes were calculated using the Barrett–Joyner–Halenda (BJH) method applied to the adsorption isotherms. FTIR spectroscopy was performed using a Bruker Vertex 80v.

2.2. Materials. Chloroform-*d* (CDCl₃, CIL; 99%), 4,4'-dimethyl-2,2'-dipyridyl (dMBpy; Aldrich; 98%), *n*-butyllithium (*n*-BuLi; Aldrich; 2.5 M in hexane), poly(ethylene glycol)-*block*-poly(propylene glycol)-*block*-poly(ethylene glycol) (EO-PO-EO; Aldrich), hydrochloric acid (HCl; ACS grade), tetraethyl orthosilicate (TEOS; Acros; 98%), (3-chloropropyl)-trimethoxysilane (CPTMS; Aldrich; 95%), hexamethyldisilazane (HMDS; Adlrich; 99%), bis(pinacolato)diboron (B₂pin₂;

Aldrich; 99%), *cis*-cyclooctene (coe; Aldrich; 95%), 4,4,5,5-tetramethyl-1,3,2-dioxaborolane (HBpin; Aldrich; 97%), methoxy(cyclooctadiene)iridium(I) dimer ([Ir(cod)(OMe)]₂; Alfa; Ir nominally 58%), 1,1,2,2-tetrachloroethane (TECE; Aldrich; 98%), acetone (ACS grade, BDH), and cyclohexane (Aldrich; 99.5%) were used as received. Arenes (Aldrich), hexane (Aldrich; >99%), methylene chloride (CH₂Cl₂; Aldrich; >99%), tetrahydrofuran (THF; Aldrich; >99%), and toluene (Aldrich, anhydrous) were dried and deoxygenated using a purification system and stored under nitrogen in a glovebox.

2.3. Preparation of Silica-Supported Bipyridine.

2.3.1. Synthesis of Bare SBA-15. To a 2 L flask, 24.0 g of EO-PO-EO, 120 mL of 38% aqueous HCl, and 635 mL of distilled water were added. The reaction mixture was kept stirring at 40 °C until the triblock copolymer template completely dissolved. Then 52.6 g of TEOS was added, and the solution was stirred overnight. The mixture was subsequently kept quiescent and heated to 100 °C for 24 h. The solid product was recovered by filtration and washed with copious amounts of DI H₂O, and air-dried overnight. The calcination of the dried material was carried out by slowly increasing the temperature from ambient to 550 °C, and then cooling back to room temperature. The solid material was further dried overnight under vacuum and stored in a glovebox.

2.3.2. Synthesis of 4'-[4-(Trimethoxysilyl)butyl]-4-methyl-2,2'-bipyridine (1). To a 250 mL flask, 1.476 g of diisopropylamine and 40 mL of dry THF were added under nitrogen; 5.43 mL of *n*-BuLi (2.5 M, 0.0132 mol) was then added dropwise to this solution at 0 °C. After the reaction mixture was kept stirring for 30 min at this temperature, a solution of 2.42 g of 4,4-dimethyl-2,2'-bipyridine (0.0132 mol) in dry THF (100 mL) was then added slowly. The remaining mixture was then allowed to keep stirring for an additional 1 h at 0 °C under nitrogen. Subsequently, a solution of 1.620 g of (3-chloropropyl)trimethoxysilane (2.41 mL, 0.0132 mol) in 10 mL of dry THF was added slowly and the solution was stirred for an additional 2 h. The reaction mixture was then allowed to warm to room temperature and stirred overnight before quenching with two drops of acetone. The remaining solvent was removed by rotovap, yielding the main product, alkoxy-silane-modified 2,2'-bipyridine as a pale yellow solid (1). It was dried under vacuum at room temperature for several hours. In this step, the product should not be washed because the alkoxy-silane-modified product is easily hydrolyzed. mp 134–138 °C. ¹H NMR (CDCl₃, 400 MHz): δ = 8.54 (m, 2H, Py), 8.20 (s, 2H, Py), 7.12 (d, *J* = 4.0 Hz, 2H, Py), 3.55 (s, 9H, OMe), 2.71 (t, *J* = 3.6 Hz, 2H, CH₂-Py), 2.43 (s, 3H, Me), 1.73 (m, 2H, CH₂), 1.58 (m, 2H, CH₂), 0.75 (t, 2H, *J* = 3.2 Hz, CH₂-Si).

2.3.3. Grafting the Bipyridine onto SBA-15 (2). A 4.0 g portion of dry SBA-15, 60 mL of toluene, and 1.6 g modified bipyridine 1 (4.62 mmol) were added to a 100 mL flask. The reaction mixture was stirred at reflux under nitrogen for 24 h. The resultant powder was filtered; washed with 80 mL each of toluene, hexane, and DCM; and dried under vacuum overnight at 100 °C. ¹³C CP-MAS NMR (100 MHz, solid state): δ = 150, 125, 48, 34, 28, 22, 12.

2.3.4. End-Capping the Functionalized SBA-15 (3). The remaining accessible silanols on the bipyridyl-functionalized SBA-15 were then capped using trimethylsilyl (-SiMe₃) groups as follows: A suspension of 2 (2.0 g) and [(CH₃)₃Si]₂NH (HMDS) (8 mL, 0.038 mol) in 25 mL dry toluene were stirred at room temperature overnight. The resultant white powder

was filtered; washed with 80 mL each of toluene, hexane, and DCM; and dried under vacuum overnight at 100 °C. ¹³C CP-MAS NMR (100 MHz, solid state): δ = 149, 124, 47, 33, 28, 21, 12, 0.1. Elemental analysis (%): C, 13.93; H, 2.29; N, 1.19; Si, 33.61.

2.4. Preparation of the Unsupported Iridium Catalyst (Ir-1).

To a 100 mL Schlenk flask, 212 mg [Ir(cod)(OMe)]₂ (0.32 mmol) and 20 mL cyclohexane were added, then 0.56 mL of *cis*-cyclooctene (4.2 mmol) was added to this solution. The yellow mixture was then kept stirring for 10 min before 0.56 mL pinacolborane (4.2 mmol) was added dropwise by syringe. Modified bipyridine 1 (222 mg, 0.64 mmol) was added as a single solid portion, and the solution was kept stirring for 45 min. Volatiles were removed by evaporation, and Ir-1 was purified by trituration with hexane to give a yellow solid (62% yield); decomposition at 140–145 °C. ¹H NMR (400 MHz, CDCl₃): δ = 9.43 (d, *J* = 5.2 Hz, 2H), 7.84 (s, 2H), 7.21 (d, *J* = 5.2 Hz, 2H), 4.20 (s, 2H), 3.54 (s, 9H, OMe), 2.70 (t, *J* = 3.6 Hz, 2H, CH₂-Py), 2.41 (s, 3H, Me), 1.72 (m, 2H, CH₂), 1.56 (m, 2H, CH₂), 1.45 (br s, 36H), 1.09 (br s, 12H), 0.73 (t, *J* = 3.2 Hz, 2H, CH₂-Si). ¹³C NMR (100 MHz, CDCl₃) δ = 155.9, 148.9, 148.2, 130.1, 124.6, 122.0, 83.4, 82.9, 74.5, 52.5, 35.1, 29.1, 26.6, 26.1, 25.4, 24.9, 24.5, 21.1. ¹¹B NMR (128 MHz, CDCl₃) δ = 22.5 (s). Elemental analysis (%): C, 48.94; H, 6.92; N, 2.64; Si, 3.21; Ir, 20.38.

2.5. Preparation of the Silica-Supported Iridium Catalyst (Ir-2).

The synthesis procedure was similar to that of Ir-1 with a slight change. To a 100 mL Schlenk flask, 60 mL of cyclohexane and 0.705 g of [Ir(cod)(OMe)]₂ (1.06 mmol) were added, then 2.0 mL of *cis*-cyclooctene (15 mmol) was added. The yellow solution was kept stirring while 2.0 mL pinacolborane (15 mmol) was added slowly. The solution turned red immediately. Then 5.0 g silica-supported bipyridine 3 was added in one portion as a white solid. The solution became dark red gradually. The flask was sealed with a rubber septum and stirred for 30 min at room temperature and then at 40 °C overnight. The solution was filtered off, and the red solid was washed with 60 mL each of cyclohexane, hexane, and DCM and dried under vacuum overnight at 100 °C. ¹³C CP-MAS NMR (100 MHz, solid state): δ = 153, 149, 124, 88, 82, 78, 68, 47, 34, 28, 21, 12, 0.1. ²⁹Si CP-MAS NMR (79.5 MHz, solid state): δ = 10.2, -63.2, -71.3, -113.6. Elemental analysis (%): C, 14.56; H, 2.48; N, 1.10; Si, 27.60; Ir, 3.79.

2.6. Direct Borylation of Arenes Catalyzed by Ir-1 and Ir-2.

In a glovebox, Ir catalyst (0.0035 mmol on the basis of iridium), bis(pinacolato)diboron (64 mg, 0.25 mmol), arene (1 mmol), and anhydrous hexane (3 mL) were added in a 10 mL glass tube with a magnetic stirring bar. The tube was then sealed with a screw cap and removed from the glovebox. After the resulting mixture was stirred at 70 °C for a designated time, *t*, the mixture was cooled to room temperature and filtered. The solvent was removed by rotovap. 1,1,2,2-Tetrachloroethane was then added to the remaining mixture as an internal standard. The yield of the product was determined by ¹H NMR on the basis of the protons in the boronate ester of the product and in B₂pin₂. The pure product was isolated by flash silica gel column chromatography (hexane/ethyl acetate = 100/0 to 90/10). Reactions were run multiple times for some substrates to minimize the impact of error in a single run, with the average yields reported in each case.

2.7. Solvent, Temperature and Ir Loading Effects on Aryl Borylation Catalyzed by Ir-2. In a glovebox, Ir-2 (designated Ir loading), bis(pinacolato)diboron (64 mg, 0.25

mmol), 1,2-dichlorobenzene (1 mmol), and anhydrous solvent (3 mL) were placed in a 10 mL glass tube with a magnetic stirring bar. The tube was then sealed with a screw cap and removed from the glovebox. After the resulting mixture was stirred at reflux for a designated time, the mixture was cooled to room temperature and filtered. The solvent was removed by rotovap. 1,1,2,2-Tetrachloroethane was then added to the remaining mixture as an internal standard. The yield of the product was determined by ^1H NMR on the basis of the protons in the boronate ester of the product and in B_2pin_2 .

2.8. Recycling Studies. In a glovebox, Ir-2 (1.0 g, 0.20 mmol on the basis of iridium), bis(pinacolato)diboron (3.6 g, 14.28 mmol), 1,2-dichlorobenzene (57 mmol), and anhydrous hexane (60 mL) were placed in a 100 mL glass tube with a magnetic stirring bar. The tube was then sealed with a screw cap and removed from the glovebox. After the resulting mixture was stirred at 70 °C for 32 h, the catalyst was separated from the reaction mixture by filtration in air. The recycled catalyst was washed with CH_2Cl_2 and hexane to remove residual organics and then was dried under vacuum at 100 °C overnight.

2.9. Kinetic Analysis of the Catalyst Ir-1, Ir-2 and Recycled Ir-2. In a glovebox, Ir catalyst (0.0035 mmol on the basis of iridium), bis(pinacolato)diboron (64 mg, 0.25 mmol), 1,2-dichlorobenzene (1 mmol), and anhydrous hexane (3 mL) were placed in a 10 mL glass tube with magnetic stirring bar. The tube was then sealed with a screw cap and removed from the glovebox. After the resulting mixture was stirred at 70 °C for a designated time, the mixture was cooled to room temperature and filtered. The solvent was removed by rotovap. 1,1,2,2-Tetrachloroethane was then added to the remaining mixture as an internal standard. The yield of the product was determined by ^1H NMR on the basis of the protons in the boronate ester of the product and in B_2pin_2 .

3. RESULTS AND DISCUSSION

3.1. Synthesis of the Iridium Catalysts. The immobilizable bipyridine ligand was prepared homogeneously according to the procedure described in the literature with some minor modification.¹⁴ A dMBpy precursor was functionalized with one of the methyl groups converted with lithium diisopropylamine to a CH_2^- anionic group, and the latter subsequently reacted with the (3-chloropropyl)trimethoxysilane to yield the immobilizable dMBpy ligand 1.

The SBA-15 materials were synthesized according to the procedure described by Brunelli et al.¹⁵ The calcined mesoporous silicate was characterized by N_2 physisorption to determine the surface area and pore size of the silica support. Powder X-ray diffraction was carried out to determine the overall structure of SBA-15. The XRD patterns (Figure 1) were consistent with a hexagonal arrangement of pores. The functionalized bipyridine was then grafted onto the SBA-15 surface by reaction with the surface silanols at reflux in toluene.¹⁶ With heating at reflux, the $-\text{Si}(\text{OCH}_3)_3$ groups react with the surface silanol groups on SBA-15 to yield the surface-tethered ligand. Filtration and elution of soluble materials and subsequent drying under vacuum afforded the bipyridine-functionalized silica gel 2. The accessible surface silanols that remained unreacted were then end-capped with a trimethylsilyl ($-\text{SiMe}_3$) group to give 3. The iridium catalysts Ir-1 and Ir-2 were synthesized by coordinating the homogeneous and immobilized bipyridine ligands with an Ir^{I} precursor, respectively. As mentioned by Hartwig and co-workers, the order of addition of HBpin and bipyridine was important to form

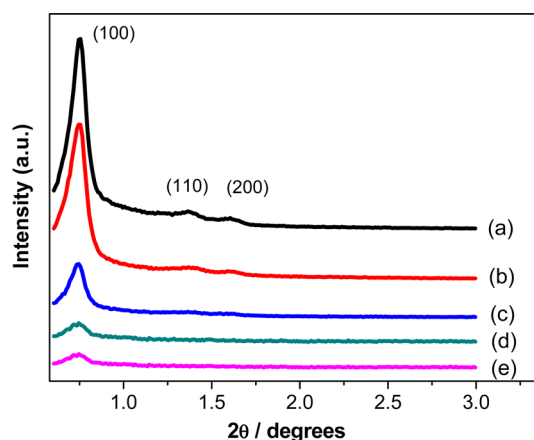


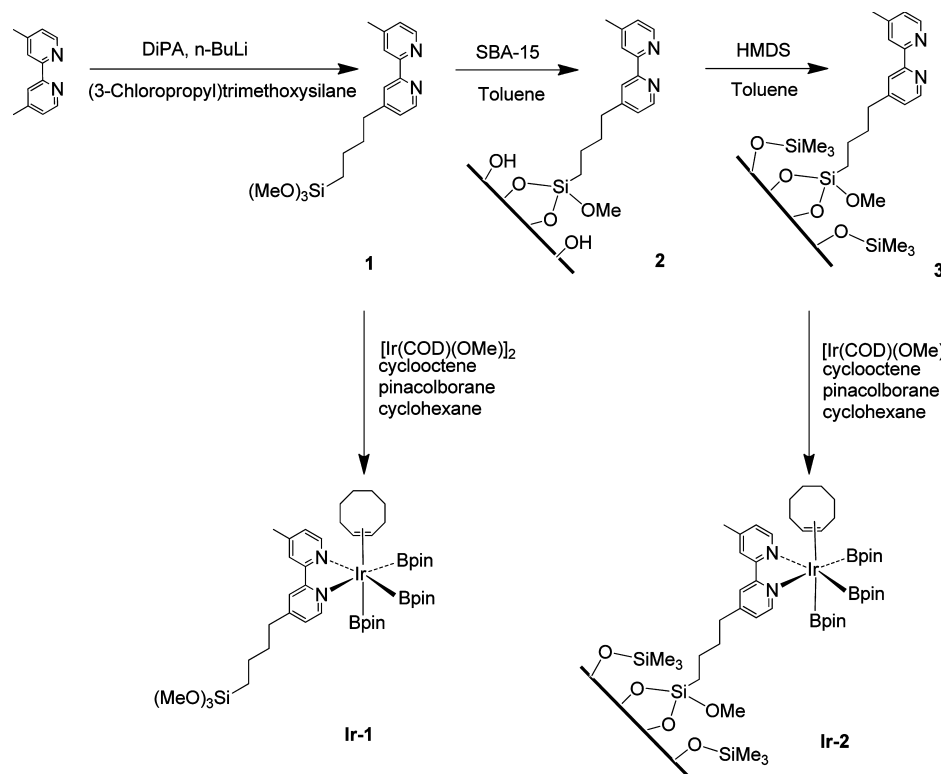
Figure 1. Powder XRD patterns of (a) SBA-15, (b) 2, (c) 3, (d) Ir-2, and (e) recycled (3 times) Ir-2.

$[\text{Ir}(\text{dtbpy})(\eta^2\text{-coe})(\text{Bpin})_3]$ in high yield.^{7c} Thus, our synthesis procedure was similar to their previous publications with some modification, in which HBpin and coe were added to the solution of $[\text{Ir}(\text{cod})(\text{OMe})_2]$ before the bipyridine ligand (Scheme 2).

3.2. Characterization of the Silica-Supported Ligands and Complexes. Figure 1 shows the low-angle XRD patterns of SBA-15 and immobilized ligands and catalysts. All the materials displayed XRD patterns with one intense diffraction peak and two weak peaks around 0.80°, 1.45°, and 1.62° indexed to (100), (110), and (200) reflections, which were characteristic of 2-D hexagonal ($P6\text{mm}$) structure, suggesting that the ordered mesostructure in pure SBA-15 was maintained after the functionalization, catalysis, and recycling.¹⁷ However, the intensity of the diffraction peaks was decreased after the grafting and complexation. This is commonly observed with such organic–inorganic hybrid materials because the presence of organic or organometallic species within the pores reduces the electron density contrast between the silicate walls and pores, reducing the intensity of the diffraction lines.¹⁸ Such a decrease in reflection intensity also provides the evidence that grafting occurs inside the mesopore channels.

The nitrogen adsorption–desorption isotherms of SBA-15 and silica-supported materials are shown in Figure 2. All the isotherms exhibited type IV behavior with H1-type hysteresis loops at high relative pressures according to IUPAC classification, which is a characteristic of capillary condensation within uniform pores.¹⁹ A sharp inflection in the P/P_0 range from 0.6 to 0.8 was found in all isotherms of the materials, providing further proof on the maintenance of the mesoporous structure after grafting and recycling.²⁰ The textural properties of the samples are summarized in Table 1. These results were in good agreement with the XRD data, which demonstrates that the mesoporous structure of SBA-15 prevailed after the immobilization of the bipyridine and complexation with Ir. The functionalized hybrid materials exhibited a considerable decrease in the BET surface area, pore volume, and pore diameter. Our results indicated that the BET surface area was 802 m^2/g for SBA-15 but decreased to 415 m^2/g for the immobilized bipyridine, and correspondingly, the pore volume shrank to 0.73 from 1.14 cm^3/g for the parent material, which was mainly due to coverage of the pore surface with the ligand.

The ^{13}C CP-MAS NMR spectra of silica-supported ligand 2 verified the presence of bipyridyl groups in the grafted material

Scheme 2. Synthetic Routes for Creation of Homogeneous and Silica-Supported Iridium Complexes^{7c;4a}

^aNote that the iridium complex is depicted without the iridium interacting with oxygen lone pairs on the surface (which could occur if the bpy or coe ligand were lost from some species) but such interactions cannot be ruled out on the basis of the data presented here.

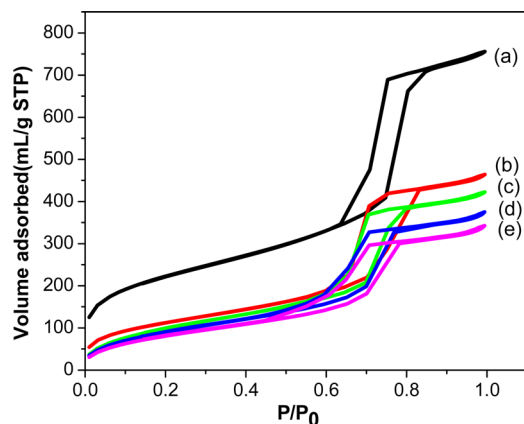


Figure 2. Nitrogen adsorption–desorption isotherms of (a) SBA-15, (b) 2, (c) 3, (d) Ir-2, and (e) recycled Ir-2.

Table 1. Textural Parameters of SBA-15 and Silica-Supported Materials Determined from N₂ Isotherms at 77 K

materials	surface area ^a (m ² /g)	pore volume ^b (cm ³ /g)	pore size ^b (nm)
SBA-15	802	1.14	6.69
2	415	0.73	6.66
3	386	0.66	5.89
Ir-2	350	0.59	5.77
recycled Ir-2	316	0.54	5.82

^aDetermined by the BET method from the adsorption branch.

^bDetermined by the BJH method from the adsorption branch.

(Figure 3). The broad peaks at 150.3 and 125.4 ppm are readily assigned to pyridyl ring carbons. The spectrum of 2 exhibited one peak at 48.7 ppm attributed to residual methoxide groups and four sharp peaks at 12.4, 22.5, 28.6, and 34.2 ppm attributed to the methylene carbons of the surface-bound alkyl spacer. All these observations are consistent with the successful postgrafting of ligands onto the mesoporous support. The new peak at 0.1 ppm in 3 does not appear in that of 2, which was assigned to the trimethylsilane groups incorporated after silanol capping, which further confirmed that the accessible residual hydroxyl groups on the silica surface were protected successfully. After complexation of the silica-supported ligand with the iridium precursor, new signals around 80 ppm appeared, as shown in the ¹³C NMR spectra of Ir-2, which are attributed to the groups of the boronate esters and cyclooctene coordinated with iridium. The presence of some boronate esters and cyclooctene interacting with the silica surface rather than the bipyridyl-ligated iridium cannot be ruled out from these spectra. The peaks of the silica-supported Ir complex Ir-2 are marked in Figure 4.

The ²⁹Si CP-MAS NMR spectrum (Figure 5) showed clearly that the silica-supported iridium complex presented a strong Q⁴ (−113 ppm) and medium T³ (−71 ppm) and T² (−63 ppm) peaks. The strong Q⁴ signal in Ir-2 indicates that the material possessed a highly condensed network structure of {Si(OSi)₄}, as expected. The relatively weak T² and T³ signals suggest the formation of {R(HO)Si(OSi)₂} and RSi(OSi)₃ (R = ligands or metal–ligand complexes), which were due to a reaction of the Si(OCH₃)₃ moiety with the −OH groups of the SBA-15 surface.¹⁷ These peaks give direct evidence of the covalent grafting of the organosilane to the silica surface. In addition, the

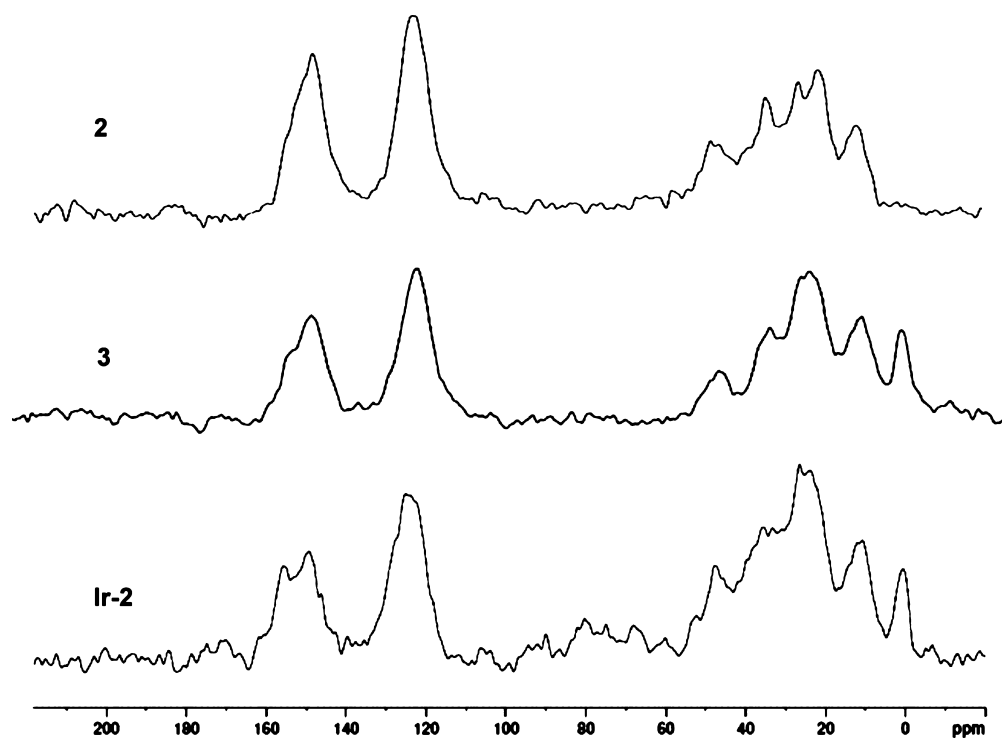


Figure 3. ^{13}C CP-MAS NMR spectra of 2, 3, and Ir-2.

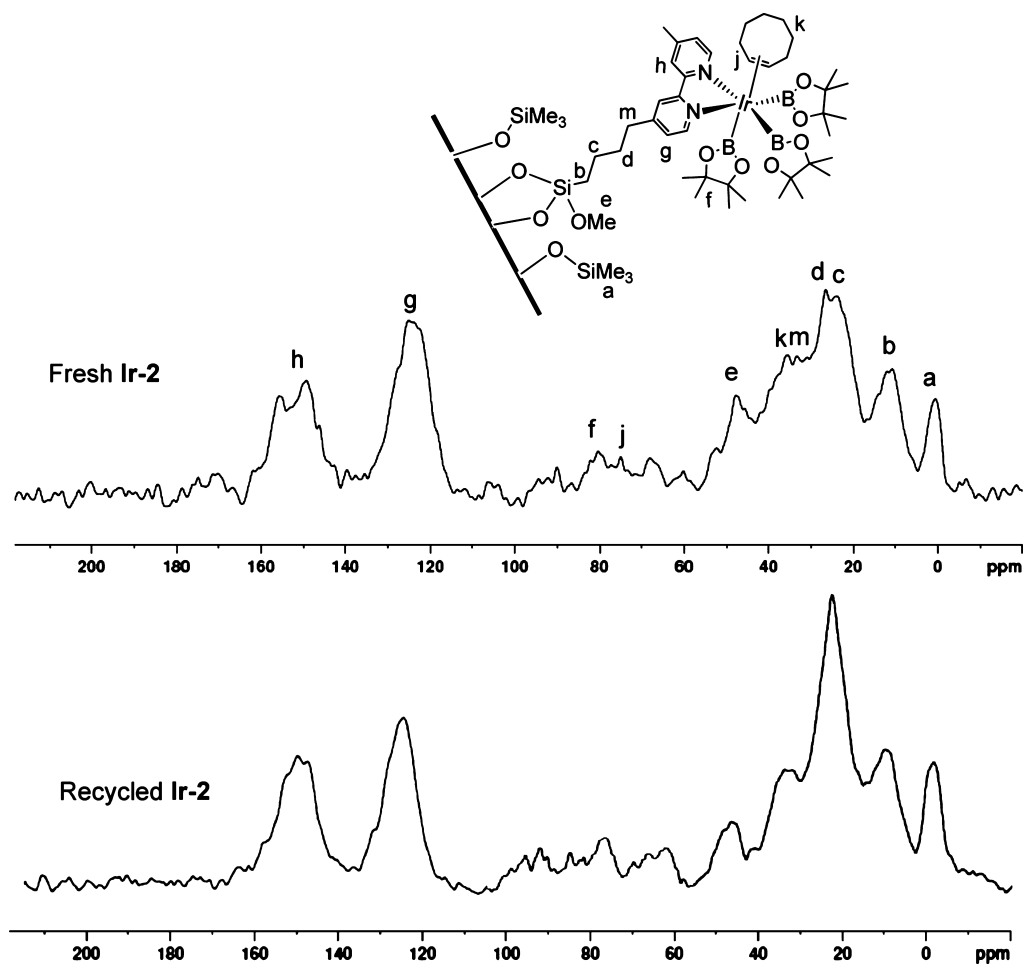


Figure 4. Comparison ^{13}C CP-MAS NMR spectra of Ir-2 and recycled Ir-2.

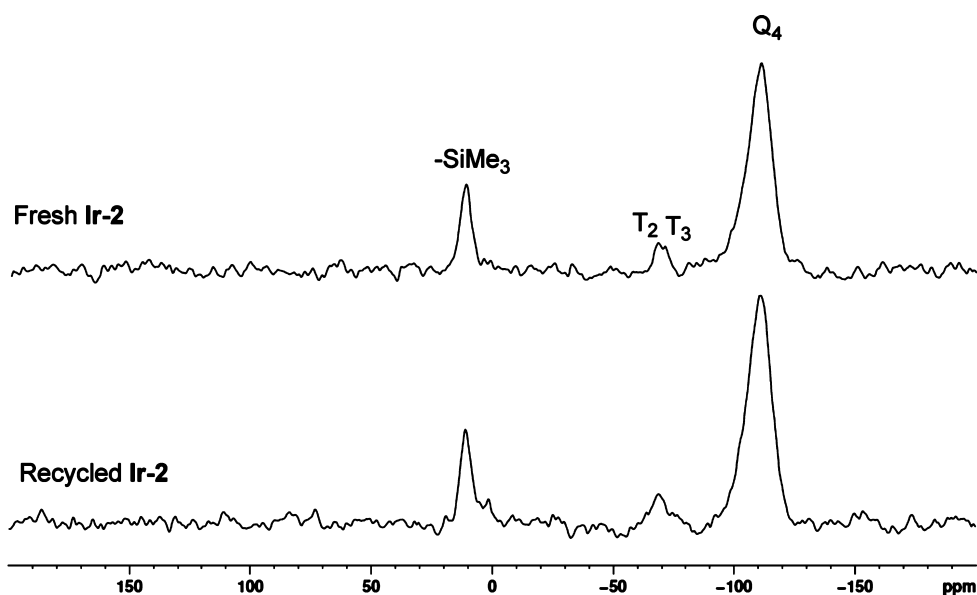


Figure 5. ^{29}Si CP-MAS NMR spectra of Ir-2 and recycled Ir-2.

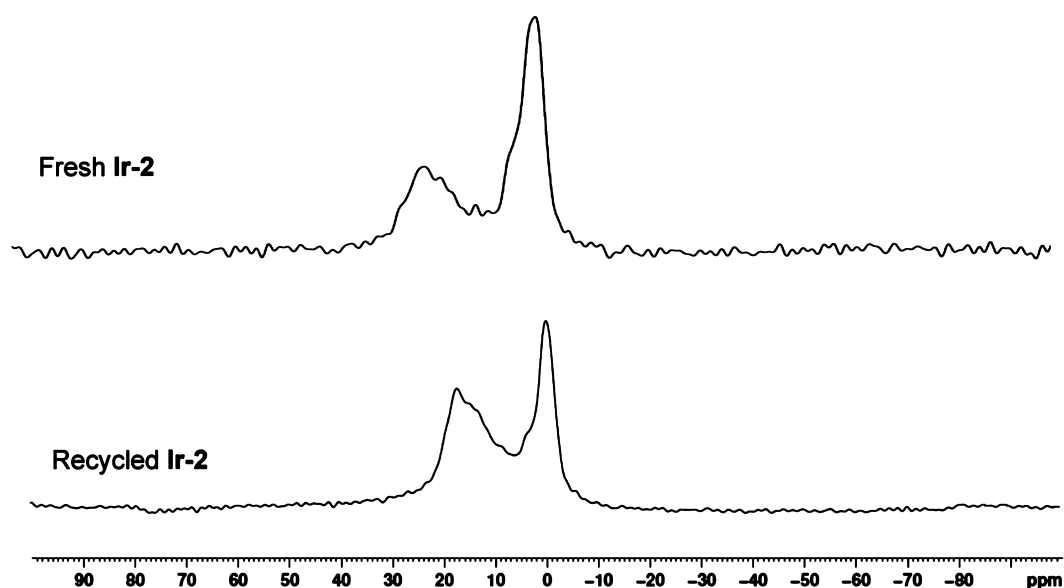


Figure 6. ^{11}B MAS NMR spectra of Ir-2 and recycled Ir-2.

^{29}Si spectrum exhibited a medium peak at 10 ppm, which was assigned to the trimethylsilane group ($\text{Si}(\text{CH}_3)_3$) introduced by the silanol protection step.²¹

As shown in Figure 6, the ^{11}B NMR spectrum of Ir-2 shows two peaks in the solid state. The chemical shift around 20 ppm falls within the expected range for boronic ester in the solid state,²² and this resonance is assigned to the boron ester group coordinated with iridium according to the related spectrum of Ir-1 in solution (Supporting Information Figure S3). Another peak around 0 ppm that did not exist in the spectrum of Ir-1 in solution is tentatively assigned to the four-coordinate ^{11}B resonance of a boron group ($\text{B}(\text{OR})_4^-$) formed due to the interaction between the boron atom of some boronate species and the silica surface ($\text{Si}-\text{O}-\text{Si}$ or $\text{Si}-\text{OH}$), since the oxygen atoms in the silica surface can donate electron density through electron lone pairs into the vacant p orbital of the boron.²² Such resonances around 0 ppm also exist in other silica-supported boron materials.²³ Additional experiments to further

elucidate the structure of the supported boron species are warranted because multiple different boron environments may exist in this material, and a more detailed study at multiple fields and via application of multinuclear NMR may shed additional light on the boron speciation.

Figure 7 displays FT-IR spectra of the SBA-15, the silica-immobilized ligands, and the supported iridium catalysts. For SBA-15 and 2, the bands at 3437 and 1632 cm^{-1} are attributed to the stretching (3437 cm^{-1}) and bending (1632 cm^{-1}) vibrations of the surface silanol groups as well as the remaining physisorbed water molecules. In addition, a band at 965 cm^{-1} is also observed in these two materials. This band can be assigned to the $\text{Si}-\text{O}$ stretching vibrations of the $\text{Si}-\text{O}-\text{H}$ groups.²⁴ All these bands became very weak or disappeared in 3 and Ir-2, indicating the hydroxyl groups on the silica surface were largely removed by ligand grafting and protection by trimethylsilyl groups. In the framework region ($400-1500\text{ cm}^{-1}$), the bands at 1085 and 806 cm^{-1} were assigned to the antisymmetric

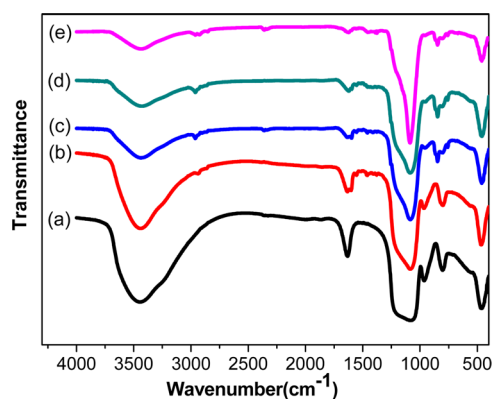


Figure 7. FT-IR spectra of (a) SBA-15, (b) 2, (c) 3, (d) Ir-2, and (e) recycled Ir-2.

stretching vibration and symmetric stretching vibration of $[\text{SiO}_4]$, and the band at 470 cm^{-1} was assigned to rocking vibrations of $[\text{SiO}_4]$.²⁵ The peaks indicative of $\nu(\text{Si}-\text{C})$ in 2, 3, and Ir-2 should appear around 1100 cm^{-1} ; however, they were difficult to distinguish because of overlap by the strong absorbance from the $\nu(\text{Si}-\text{O})$ band. Weak bands of 2, 3, and Ir-2 at 2800 cm^{-1} were assigned to asymmetric and symmetric stretching vibrations of $-\text{CH}_2-$ bonds, and the bands around 1620 cm^{-1} were attributed to breathing vibrations of $\text{C}=\text{C}$ bonds of the aromatic rings. In addition, the weak bands at 1480 and 780 cm^{-1} represent $-\text{CH}_2-$ bending and $-\text{CH}_2-$ rocking modes, respectively.²⁶ All these relatively weak bands derived from the ligands or metal complexes suggest successful incorporation of the intended species into the mesoporous silica materials, which was further supported by the solid-state NMR spectra discussed above.

The elemental analysis data of the silica-supported ligand and iridium complexes are listed in Table 2. These demonstrate

Table 2. Elemental Analysis Results for the Immobilized Ligand and Complex

entry	samples	% C	% H	% N	% Si	% Ir
1	3	13.93	2.29	1.19	33.61	
2	Ir-2 fresh	14.56	2.48	1.10	27.60	3.79
3	Ir-2 after 1st use	14.99	2.53	1.02	28.12	3.68
4	Ir-2 after 2nd use	15.21	2.24	1.04	24.07 ^a	3.63

^aThis % Si value might be inaccurate, given the consistency of all the other data.

very little change of metal content after recycling, suggesting good stability of the supported complex. Moreover, the ligand loading of the materials calculated from TGA (Supporting Information Figure S1) was similar to that from the elemental microanalysis, as shown in Table 3. The overestimation of the ligand content via TGA is likely due to some loss of silanols (on the surface or buried within the silica walls) via condensation at high temperatures, with this weight loss falsely ascribed to organic species. The L/Ir ratios (Table 3) suggest that uncoordinated bipyridine ligands must exist and that about half of the ligands were initially involved in the metalation with Ir.

It should be noted that the elemental analysis and IR and NMR spectroscopic results are consistent with the creation of the intended supported species as depicted in Scheme 2, although the presence of bipyridines that are not coordinated

Table 3. Ligand and Iridium Loading of the Immobilized Materials

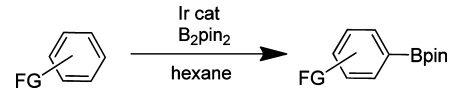
entry	samples	L loading ^a (mmol/g cat)	L loading ^b (mmol/g cat)	Ir loading ^c (mmol/g cat)	(L/Ir) ^d (mole ratio cat)
1	3	0.52	0.43		
2	Ir-2 fresh	0.45	0.39	0.20	1.95
3	Ir-2 after 1st use	0.48	0.36	0.19	1.89
4	Ir-2 after 2nd use	0.44	0.37	0.19	1.94

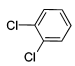
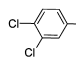
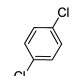
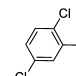
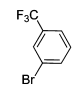
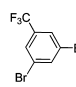
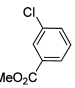
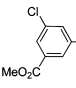
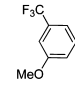
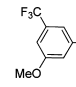
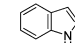
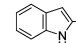
^aBased on thermogravimetric analysis. ^bBased on total nitrogen content by CHN elemental analysis. ^cBased on total iridium content by ICP-AES elemental analysis. ^dMolar ratio of ligand to iridium based on element analysis.

with iridium also exist on the surface. In addition, the presence of some iridium species interacting with the silica surface via oxygen lone pairs (after loss of *coe* or *bpy* species) cannot be ruled out on the basis of the ¹¹B spectrum of heterogeneous catalyst.

3.3. C–H Borylation of Arenes. With the supported iridium complex Ir-2 in hand, its ability to catalyze aromatic C–H borylation reactions was examined. The unsupported iridium complex Ir-1 was also used in these catalytic processes for comparison. The borylation was carried out in hexane solution at reflux, with a slight excess of substrate to B_2pin_2 to avoid multiple borylation of the arenes. The catalytic results obtained from the borylation of various arenes are summarized in Table 4. In all cases, the borylation occurred at C–H bonds located meta or para to a substituent in preference to those located in the ortho position. Thus, the reactions occurred regioselectively with disubstituted arenes. Both 1,2- and 1,4- dichlorobenzenes yielded the corresponding boronate ester as a single product (Table 2, entries 1 and 2). The yields for reaction of the 1,4- isomer were lower than for 1,2- isomer, which was probably due to the steric hindrance. Isomerically pure products were obtained in moderate to good yields, even with two distinct substituents on arenes (Table 4, entries 3–5). In addition, electron-withdrawing substituents activated the arene for the borylation process, as shown by the catalytic results from entries 3–5 (Table 4). Functional group tolerance of the borylation reaction is higher than in boronate synthesis through magnesium or lithium reagents.²⁷ The reaction was suitable for arenes possessing a wide variety of functional groups, such as Cl, Br, CF_3 , OMe, and CO_2Me . The aryl bromide underwent borylation at the C–H bond (entry 3) without C–X bond cleavage. In the case of indole, the borylation selectively occurred at the α -position to form a single isomer in 90% yield for Ir-1 and 72% for Ir-2 (Table 4, entry 6).

A comparison of the catalytic activity of the homogeneous catalyst (Ir-1) and its immobilized counterpart (Ir-2) showed an activity reduction in most cases, which could be due to lower accessibility of the active sites within the pores of SBA-15. For example, for the substrates with electron-donating groups (entry 5), the supported complex behaved poorly compared with the homogeneous catalyst; however, the heterogeneous catalyst (Ir-2) exhibited similar or even better catalytic performance relative to the homogeneous analogue (Ir-1) when choosing 1,2-dichlorobenzene (entry 1) or 1-trifluoromethyl-3-bromobenzene (entry 3) as the substrate. A high turnover number (TON of 136) of the heterogeneous catalyst

Table 4. Ir-Catalyzed Direct Borylation of Arenes with B_2pin_2 ^a


Entry	Substrate	Product	Ir-1		Ir-2	
			Time (h)	Yield ^b (%)	Time (h)	Yield ^{b,c} (%)
1			8	96 (100,94,95)	24	95 (97,94)
2			24	30	48	10 (9, 12)
3			12	63	24	92 (94,91)
4			12	57 (61,54)	32	27
5			24	53	48	12 (10,14)
6			12	90	32	72

^aA mixture of B_2pin_2 (0.25 mmol), an arene (1.0 mmol), and Ir catalyst (0.0035 mmol on the basis of iridium) was stirred in hexane (3 mL) at 70 °C for the period shown in the Table. ^bThe average ¹H NMR yields are calculated on the basis of the protons of the Bpin group in the product and in B_2pin_2 . The data in parentheses are the yields obtained in duplicate runs.

(Ir-2) was attained, which was comparable to the homogeneous catalyst $1/2[\{Ir(OMe)(cod)\}_2]/dtbpy$ (TON of 67)⁵ or the silica-SMAP-Ir(OMe)(cod) (TON of 200)¹⁰ under similar conditions. A higher turnover number was reported by Hartwig (TON of 8000) and Sawamura (TON of 20000) using more extreme conditions where the reactions were carried out in the presence of a large excess of substrate to B_2pin_2 at high temperature (100 °C).^{5,10}

The reaction solvent was reported by many groups to have an effect on the activity of the catalyst.^{7d} For example, Ishiyama and co-workers reported that the activity of their homogeneous catalysts for borylations was much lower in polar solvents relative to that in hexane.²⁸ To verify whether the supported catalyst showed similar behavior, other borylation experiments were carried out with DCM, acetonitrile, and THF as solvents. As shown in Table 5, the supported catalyst was not effective for aryl borylation in polar solvents. No product was observed when the experiment was run in DCM or acetonitrile. Only 12% yield was obtained when THF was used, even if the reaction was carried out for a prolonged period of time. Thus, the order of reactivity in different solvents was hexane (95%) > THF (12%) > DCM (0%) = acetonitrile (0%), which is consistent with that of the typical homogeneous catalyst.^{28a}

The influence of the temperature and catalyst loading on the activity of the catalyst was also evaluated. The results of entries 3, 8, and 9 in Table 5 demonstrate that an increased reaction temperature led to improved yields (in hexane solution). The data presented in entries 1–4 (Table 5) show that an increased

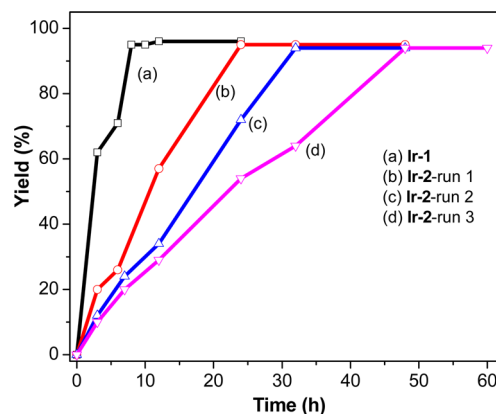
Table 5. Aromatic Borylation Catalyzed by Ir-2 in Different Solvents^a

entry	cat. (mol %) ^b	solvent	T (°C)	time (h)	yield (%) ^c
1	0.5	hexane	70	48	24
2	0.9	hexane	70	48	77
3	1.4	hexane	70	24	95
4	1.8	hexane	70	24	95
5	1.8	DCM	40	48	
6	1.8	THF	70	48	12
7	1.8	acetonitrile	80	48	
8	1.4	hexane	25	48	4
9	1.4	hexane	45	48	28

^aA mixture of B_2pin_2 (0.25 mmol), 1,2-dichlorobenzene (1.0 mmol), and Ir-2 was stirred in solvent (3 mL) for the period shown in the Table. ^bThe mole ratio of iridium to B_2pin_2 . ^c¹H NMR yields are based on the protons of the Bpin group in the product and in B_2pin_2 .

amount of catalyst led to higher activity. The lowest tested catalyst loading was 0.5 mol %, and only low yields (24% after 48 h, entry 1) were observed with this small amount of catalyst. The highest yield was attained when the iridium loading was elevated to 1.4 mol %. However, there was no increase in the yield if additional catalyst was added beyond this loading. All of these trends are typical, showing no unexpected deviations of behavior of this catalyst relative to homogeneous versions.

Although reaction yields at long times are useful information for synthetic purposes, to assess the utility of the catalyst, it is best to gather kinetic profiles for the reactions. To this end, kinetic experiments were performed for the borylation of 1,2-dichlorobenzene with B_2pin_2 to compare the activity of the catalysts, as shown in Figure 8. The kinetic profiles revealed

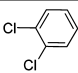
**Figure 8.** Kinetic analysis of the borylation of 1,2-dichlorobenzene catalyzed by iridium complexes.

that the borylation catalyzed by the homogeneous Ir-1 (initial TOF = 17.2 h⁻¹) occurred at a higher rate than that of Ir-2 (initial TOF = 6.5 h⁻¹), indicating a higher activity for the unsupported catalyst. The decrease in the activity may be because a fraction of the supported Ir is inactive in the reaction, leading to TOFs being lower for the supported catalyst. This may be due to unfavorable interactions of the iridium center with the silica surface or possible decomposition of some fraction of the iridium complexes tethered to the surface. Indeed, ¹¹B NMR evidence may suggest that the complex is altered to some degree upon addition to the silica support. However, a definitive explanation for the slower rates over the heterogeneous catalyst will require a more extensive structural

investigation of the catalyst focusing on the coordination sphere of the iridium and boron centers.

After being simply filtered from the reaction media and washed with CH_2Cl_2 , Ir-2 could be used repetitively several times for the aryl borylation with B_2pin_2 , as shown in Table 6

Table 6. Recycling Studies of Ir-2 in Borylation of 1,2-Dichlorobenzene^a

Substrate	cycle	Yield ^b (%)			Initial TOF (h ⁻¹)
		12 h	24 h	48 h	
	1	57	95	95	6.5
	2	34	72	94	4.0
	3	29	54	94	3.4

^aA mixture of B_2pin_2 (0.25 mmol), 1,2-dichlorobenzene (1.0 mmol), and Ir-2 (0.0035 mmol on the basis of iridium) was stirred in hexane (3 mL) at 70 °C. ^b¹H NMR yields are based on the protons of the Bpin group in the product and in B_2pin_2 .

and Figure 8. Although the initial TOF of the catalyst was gradually decreased upon recycling, which is typical of supported catalysts, the recycled catalyst still afforded 94% yield after two cycles when using 1,2-dichlorobenzene as the substrate. The time required to achieve 94% yield increased from 24 to 48 h over three runs. It should be noted that no regeneration of the catalyst with an iridium precursor or boron reagent was carried out between the individual runs. These results indicate that the silica-supported iridium catalyst Ir-2 possessed good efficiency and recyclability in the aromatic C–H borylation reaction.

To verify that the observed catalysis was due to silica-supported rather than leached iridium species in solution, a hot filtration experiment was carried out. As shown in Figure 9, the

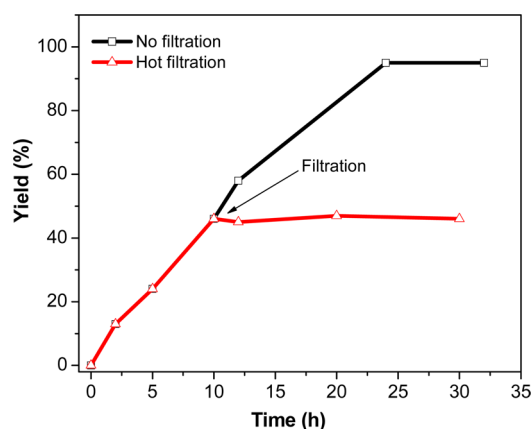


Figure 9. Hot filtration test for the Ir-2 catalyzed borylation reaction of 1,2-dichlorobenzene and B_2pin_2 with hexane at 70 °C. The solid catalyst was filtered off after 10 h in the run represented by red triangles.

heterogeneous catalyst Ir-2 was filtered from the reaction mixture after 10 h, and the reaction was continued for an additional 20 h. It was found that there was no appreciable change in the yield of the product after the solid catalyst was removed, and the solid-free solution was colorless. This observation eliminated the possible catalytic role of homogeneous iridium species, confirming that the recycle efficiency was derived from the heterogeneous catalyst itself. This finding was consistent with the results of the elemental analysis, which

showed that the L/Ir ratio of the recycled catalyst was relatively constant over the recycles, as shown in Table 3. Similarly, the filtered solid from the recycling test was also characterized by solid state NMR spectroscopy, IR spectroscopy, nitrogen physisorption, XRD, and TGA (see above). All the results were very similar to those of the fresh catalyst, with minor reductions in porosity and increases in residual organic content, indicating that the mesostructure of the SBA-15 and supported metal complex were well preserved after the catalytic reaction. Thus, the gradual decrease in the catalytic activity during the recycle was associated not with leaching of iridium metal, but rather, with other reasons, such as the loss of boronate ester groups, loss of pore volume and surface area due to desposition of organic species in the pores during the reactions, or both. Future studies should focus on elucidating the mechanisms that lead to loss of activity upon recycle.

4. CONCLUSIONS

In summary, we have successfully prepared a mesoporous silica-supported bipyridine iridium complex Ir-2 for direct C–H borylation of arenes. This is the first reported supported analogue of Hartwig's $1/2[\{\text{Ir}(\text{OMe})(\text{cod})\}_2]/\text{dtbpy}$ catalyst. Both the unsupported catalyst and supported catalyst showed moderate to good activity for various arenes containing different kinds of functional groups. The supported catalyst exhibited a comparable TON relative to a typical homogeneous catalyst $1/2[\{\text{Ir}(\text{OMe})(\text{cod})\}_2]$ or silica-SMAP-Ir-(OMe)(cod) developed by Hartwig (homogeneous) and Sawamura (supported) under similar conditions. More importantly, the heterogeneous catalyst was stable in air and could be recovered by simple filtration and used repetitively with only a modest decrease in catalytic rate. For example, the use of the recycled catalyst for C–H borylation of 1,2-dichlorobenzene produced the desired product in very high yield over multiple cycles. The structural characterization of the fresh and recycled catalyst suggested that the integrity of both the metal complex and the inorganic support were retained in consecutive catalytic runs, showing good potential for application in practical synthesis in which high TONs are desired.

■ ASSOCIATED CONTENT

Supporting Information

Additional experimental details and material characterization data as noted in text. This material is available free of charge via the Internet at <http://pubs.acs.org>.

■ AUTHOR INFORMATION

Corresponding Author

*E-mail: cjones@chbe.gatech.edu.

Author Contributions

[§]F.W. and Y.F. contributed equally to this work.

Notes

The authors declare no competing financial interest.

■ ACKNOWLEDGMENTS

This research was supported by the National Science Foundation under the Center for Chemical Innovation in Stereoselective C–H Functionalization (CHE-1205646). F. Wu gratefully acknowledges the financial support of the China Scholarship Council (CSC).

REFERENCES

- (1) (a) Hartwig, J. F. *Acc. Chem. Res.* **2012**, *45*, 864–873. (b) Liu, T.; Shao, X.; Wu, Y.; Shen, Q. *Angew. Chem., Int. Ed.* **2012**, *51*, 540–543. (c) Liskey, C. W.; Liao, X.; Hartwig, J. F. *J. Am. Chem. Soc.* **2010**, *132*, 11389–11391. (d) Murphy, J. M.; Liao, X.; Hartwig, J. F. *J. Am. Chem. Soc.* **2007**, *129*, 15434–15435. (e) Tzschucke, C. C.; Murphy, J. M.; Hartwig, J. F. *Org. Lett.* **2007**, *9*, 761–764. (f) Partridge, B. M.; Hartwig, J. F. *Org. Lett.* **2013**, *15*, 140–143.
- (2) Cho, J. Y.; Tse, M. K.; Holmes, D.; Maleczka, R. E., Jr.; Smith, M. R., III. *Science* **2002**, *295*, 305–308.
- (3) Iverson, C. N.; Smith, M. R., III. *J. Am. Chem. Soc.* **1999**, *121*, 7696–7697.
- (4) (a) Ishiyama, T.; Isou, H.; Kikuchi, T.; Miyaura, N. *Chem. Commun.* **2010**, *46*, 159–161. (b) Chotana, G. A.; Vanchura, B. A., II; Tse, M. K.; Staples, R. J.; Maleczka, R. E., Jr.; Smith, M. R., III. *Chem. Commun.* **2009**, 5731–5733. (c) Ishiyama, T.; Miyaura, N. *Pure Appl. Chem.* **2006**, *78*, 1369–1375. (d) Ishiyama, T.; Takagi, J.; Yonekawa, Y.; Hartwig, J. F.; Miyaura, N. *Adv. Synth. Catal.* **2003**, *345*, 1103–1106. (e) Roosen, P. C.; Kallepalli, V. A.; Chattopadhyay, B.; Singleton, D. A.; Maleczka, R. E., Jr.; Smith, M. R., III. *J. Am. Chem. Soc.* **2012**, *134*, 11350–11353.
- (5) Ishiyama, T.; Takagi, J.; Ishida, K.; Miyaura, N.; Anastasi, N. R.; Hartwig, J. F. *J. Am. Chem. Soc.* **2002**, *124*, 390–391.
- (6) Mkhaliid, I. A.; Barnard, J. H.; Marder, T. B.; Murphy, J. M.; Hartwig, J. F. *Chem. Rev.* **2010**, *110*, 890–931.
- (7) (a) Dai, C. Y.; Stringer, G.; Marder, T. B.; Scott, A. J.; Clegg, W.; Norman, N. C. *Inorg. Chem.* **1997**, *36*, 272–273. (b) Nguyen, P.; Blom, H. P.; Westcott, S. A.; Taylor, N. J.; Marder, T. B. *J. Am. Chem. Soc.* **1993**, *115*, 9329–9330. (c) Boller, T. M.; Murphy, J. M.; Hapke, M.; Ishiyama, T.; Miyaura, N.; Hartwig, J. F. *J. Am. Chem. Soc.* **2005**, *127*, 14263–14278. (d) Preshlock, S. M.; Ghaffari, B.; Maligres, P. E.; Krska, S. W.; Maleczka, R. E., Jr.; Smith, M. R., III. *J. Am. Chem. Soc.* **2013**, *135*, 7572–7582.
- (8) (a) Zhu, Y.; Yan, K.; Luo, J.; Chong, S. H.; Yong, C. H.; Emi, A.; Su, Z.; Monalisa, W.; Narayan, S. H.; John, A. M. *J. Organomet. Chem.* **2007**, *692*, 4244–4250. (b) Zhu, Y.; Koh, C.; Ang, T. P.; Emi, A.; Winata, M.; Loo, K. J. L.; Narayan, S. H.; John, A. M. *Inorg. Chem.* **2008**, *47*, 5756–5761.
- (9) (a) Tagata, T.; Nishida, M.; Nishida, A. *Tetrahedron. Lett.* **2009**, *50*, 6176–6179. (b) Tagata, T.; Nishida, M.; Nishida, A. *Adv. Synth. Catal.* **2010**, *352*, 1662–1666.
- (10) Kawamorita, S.; Ohmiya, H.; Hara, K.; Fukuoka, A.; Sawamura, M. *J. Am. Chem. Soc.* **2009**, *131*, 5058–5059.
- (11) (a) Yamazaki, K.; Kawamorita, S.; Ohmiya, H.; Sawamura, M. *Org. Lett.* **2010**, *12*, 3978–3981. (b) Kawamorita, S.; Ohmiya, H.; Sawamura, M. *J. Org. Chem.* **2010**, *75*, 3855–3858.
- (12) Kawamorita, S.; Miyazaki, T.; Ohmiya, H.; Iwai, T.; Sawamura, M. *J. Am. Chem. Soc.* **2011**, *133*, 19310–19313.
- (13) Geier, M. J.; Geier, S. J.; Vogels, C. M.; B eland, F.; Westcott, S. A. *Synlett* **2009**, *3*, 477–481.
- (14) (a) Nguyen, J. V.; Jones, C. W. *Macromolecules* **2004**, *37*, 1190–1203. (b) Sun, L.; Mai, W.; Dang, S.; Qiu, Y.; Deng, W.; Shi, L.; Yan, W.; Zhang, H. *J. Mater. Chem.* **2012**, *22*, 5121–5127.
- (15) Brunelli, N. A.; Didas, S. A.; Venkatasubbaiah, K.; Jones, C. W. *J. Am. Chem. Soc.* **2012**, *134*, 13950–13953.
- (16) Ping, E. W.; Venkatasubbaiah, K.; Fuller, T. F.; Jones, C. W. *Top. Catal.* **2010**, *53*, 1048–1054.
- (17) Zhao, D.; Hu, Q.; Feng, J.; Chmelka, B. F.; Stucky, G. D. *J. Am. Chem. Soc.* **1998**, *120*, 6024–6036.
- (18) Hicks, J. C.; Drese, J. H.; Fauth, D. J.; Gray, M. L.; Qi, G.; Jones, C. W. *J. Am. Chem. Soc.* **2008**, *130*, 2902–2903.
- (19) Gregg, S. J.; Sing, K. S. W. *Adsorption, Surface Area and Porosity*, 2nd ed.; Academic Press: London, 1982.
- (20) Yang, L. N.; Qi, Y. T.; Yuan, X. D.; Shen, J.; Kim, J. *J. Mol. Catal. A* **2005**, *229*, 199–205.
- (21) Sayah, R.; Framery, E.; Dufaud, V. *Green Chem.* **2009**, *11*, 1694–1702.
- (22) Weiss, J. W.; Bryce, D. L. *J. Phys. Chem. A* **2010**, *114*, 5119–5131.
- (23) Gunther, W. R.; Wang, Y.; Ji, Y.; Michaelis, V. K.; Hunt, S. T.; Griffin, R. G.; Roman-Leshkov, Y. *Nat. Commun.* **2012**, *3*, 1109.
- (24) Luan, Z.; Fournier, J. A. *Microporous Mesoporous Mater.* **2005**, *79*, 235–240.
- (25) Zaki, M. I.; Fouad, N. E.; Leyrer, J.; Knozinger, H. *Appl. Catal.* **1986**, *21*, 359–377.
- (26) Doadrio, J. C.; Sousa, E. M. B.; Izquierdo-Barba, I.; Doadrio, A. L.; Vallet-Regi, M. J. *Mater. Chem.* **2006**, *16*, 462–466.
- (27) (a) Pelter, A.; Smith, K.; Brown, H. C. *Borane Reagents*; Academic Press: London, 1988; p 434. (b) Nesmeyanov, A. N.; Sokolik, R. A. *Methods of Elemento-Organic Chemistry*; North-Holland: Amsterdam, 1967; Vol. 1, p 551.
- (28) (a) Ishiyama, T.; Takagi, J.; Hartwig, J. F.; Miyaura, N. *Angew. Chem., Int. Ed.* **2002**, *41*, 3056–3058. (b) Ishiyama, T.; Nobuta, Y.; Hartwig, J. F.; Miyaura, N. *Chem. Commun.* **2003**, 2924–2925.